IOPscience iopscience.iop.org

Home Search Collections Journals About Contact us My IOPscience

Flexible relaxor materials: $Ba_2Pr_xNd_{1-x}FeNb_4O_{15}$ tetragonal tungsten bronze solid solution

This article has been downloaded from IOPscience. Please scroll down to see the full text article.

2009 J. Phys.: Condens. Matter 21 452201

(http://iopscience.iop.org/0953-8984/21/45/452201)

View the table of contents for this issue, or go to the journal homepage for more

Download details:
IP Address: 129.252.86.83
The article was downloaded on 30/05/2010 at 06:00

Please note that terms and conditions apply.

IOP FTC
IOP PUBLISHING JOURNAL OF PHYSICS: CONDENSED MATTER
J. Phys.: Condens. Matter **21** (2009) 452201 (5pp) doi:10.1088/0953-8984/21/45/452201

FAST TRACK COMMUNICATION

Flexible relaxor materials: $Ba_2Pr_xNd_{1-x}FeNb_4O_{15}$ tetragonal tungsten bronze solid solution

Elias Castel, Michaël Josse, Dominique Michau and Mario Maglione[1]

ICMCB-CNRS, 87 avenue du Docteur Schweitzer, F-33608 Pessac Cedex, France

E-mail: maglione@icmcb-bordeaux.cnrs.fr

Received 2 July 2009, in final form 27 September 2009
Published 9 October 2009
Online at stacks.iop.org/JPhysCM/21/452201

Abstract
Relaxors are very interesting materials but most of the time they are restricted to perovskite materials and thus their flexibility is limited. We have previously shown that tetragonal tungsten bronze (TTB) niobate $Ba_2PrFeNb_4O_{15}$ was a relaxor below 170 K and that $Ba_2NdFeNb_4O_{15}$ displays a ferroelectric behavior with a $T_C = 323$ K. On scanning the whole solid solution $Ba_2Pr_xNd_{1-x}FeNb_4O_{15}$ ($x = 0$, 0.2, 0.4, 0.5, 0.6, 0.8 and 1), we demonstrate here a continuous crossover between these end member behaviors with a coexistence of ferroelectricity and relaxor in the intermediate range. This tunability is ascribed to the peculiar structure of the TTB networks which is more open than the classical perovskites. This allows for the coexistence of long range and short range orders and thus opens up the range of relaxor materials.

(Some figures in this article are in colour only in the electronic version)

Because of their useful dielectric and piezoelectric properties, relaxors are undergoing thorough investigation at present [1–3]. Currently, most relaxors belong to the perovskite family and a lot of these contain lead ions. We already showed that lead-free perovskites are more flexible than lead-containing ones because a continuous crossover from ferroelectric to relaxor is observed in many solid solutions [4, 5]. A possible coexistence of ferroelectric and relaxor states in the same material would be a step further in favor of lead-free materials. In the case of a close packed perovskite structure such a coexistence has already been reported in sodium bismuth titanate-based compositions $Na_{0.5}Bi_{0.5}TiO_3$ [6, 7] or in the $BaTiO_3$ family, like $Ba_{0.9}Bi_{0.067}(Ti_{1-x}Zr_x)O_3$ ceramics [8]. The origin of such a coexistence in these bismuth-containing materials is, however, still a matter of debate.

We show here that a more open crystalline network, like the so-called tetragonal tungsten bronze structure, is able to trigger such a coexistence in a much more obvious way. As shown in figure 1, the TTB structure is based on interconnected octahedra, leaving three different channels of threefold, fourfold and fivefold pseudo-symmetry. Numerous cations can be hosted within such channels, thus opening up a wide range of interesting compositions [9, 10]. Starting from $Ba_{2,5}Nb_5O_{15}$ where only the fourfold and fivefold channels are occupied by barium, it was already shown that the fourfold channels may be filled by a lanthanide ion (Ln) provided that a related amount of Fe is substituted to Nb within the octahedra for the sake of preserving the overall lattice neutrality. The resulting $Ba_2LnFeNb_4O_{15}$ has appealing properties, including composite multiferroics at room temperature [11, 12].

Here, we want to show that, when the rare earth cationic site is occupied by a mixture of praseodymium (Pr) and neodymium (Nd), a continuous solid solution is obtained which exhibits very interesting behaviors when scanning the composition from Nd to Pr. First, the high temperature ferroelectric transition, which is a common feature of a lot of TTBs, just collapses without a significant shift of the transition temperature. At the same time, a low temperature relaxor state grows and ferroelectricity is totally suppressed in the Pr pure

[1] Author to whom any correspondence should be addressed.

 © 2009 IOP Publishing Ltd Printed in the UK

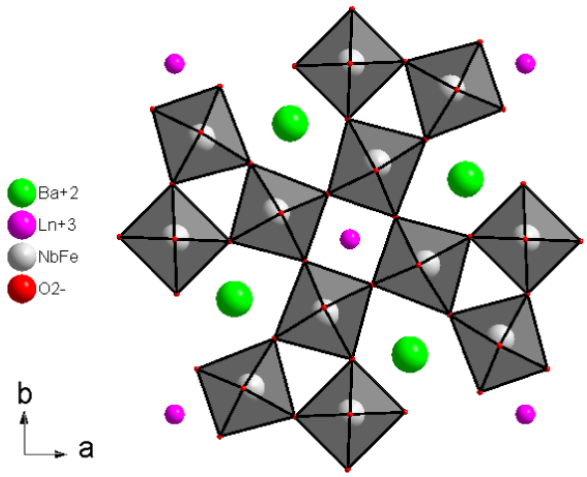

Figure 1. Crystal structure of $Ba_2LnFeNb_4O_{15}$ viewed along the c axis. The Ba and Ln cations occupy the fivefold and fourfold sites, respectively, while the ferroelectric active Nb cations are sited at the center of the oxygen octahedron.

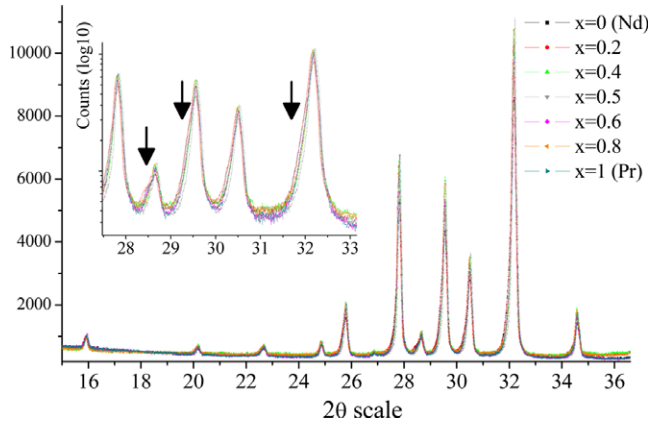

Figure 2. XRD patterns for $Ba_2Pr_xNd_{1-x}FeNb_4O_{15}$ ($x = 0$, 0.2, 0.4, 0.5, 0.6, 0.8, and 1) ceramics. Arrows are drawn in the XRD patterns inset plotted on a semilogarithmic scale to emphasis the $LnNbO_4$ secondary phase which is independent of x.

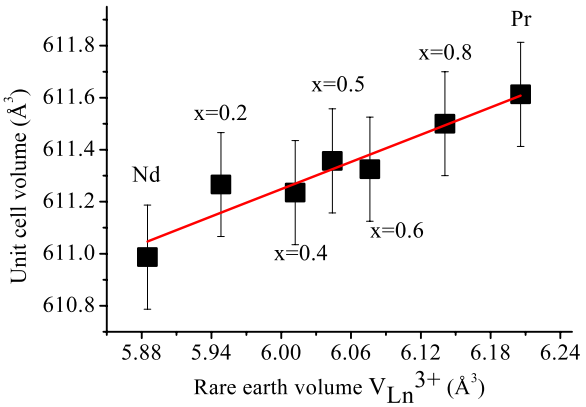

Figure 3. The unit cell volume plotted versus the equivalent rare earth ionic volume V_{Ln}^{3+}.

compound. These features, which are hardly observed in other ferroelectric materials like perovskites [13], will be discussed in view of the specific structure of the TTB network.

Before describing the dielectric data, we summarize briefly all the processing, shaping and characterization that we undertook to ensure high quality and reproducible ceramics. These important steps will be described in more detail elsewhere. After optimized synthesis and sintering, powder x-ray diffraction showed a pure TTB phase for all compositions $Ba_2Nd_{1-x}Pr_xFeNb_4O_{15}$ from $x = 0$ to 1 with no spurious phase in the limit of 0.5% (figure 2). The symmetry for all powders was tetragonal $P4/mbm$ at room temperature. The lattice parameters and unit volume of these TTB changed continuously following Vegard's law which states that the lattice parameters of the solid solution are a linear combination of the end members. In figure 3, we show that the unit cell volume is linearly increasing when the composition changes from Nd to Pr. On the x axis of this Vegard law, we have reported the equivalent rare earth ionic volume instead of the praseodymium content x. This is to show that the unit cell volume is directly proportional to the effective ionic size at the A site of the TTB structure.

X-ray microprobe analysis confirmed that the amount of spurious phases is only marginal and that it is independent of the given composition x. These first observations confirm that all changes in the dielectric properties do not originate from uncontrolled segregation of phases. In addition, scanning electron microscopy showed that the shape and size distribution of grains in the final ceramics were similar over all the solid solution and the porosity was low. In particular we observed the mean grain size of all our ceramics stays constant to about 20 ± 10 μm. The compactness of all the studied pellets was better than 92% as computed from density measurements.

Dielectric measurements were performed on ceramic discs (8 mm diameter, 1 mm thickness) after deposition of gold electrodes on the circular faces by cathodic sputtering. The real and imaginary relative permittivities ε_r' and ε_r'' were determined under dry helium as a function of both temperature (77–420 K) and frequency (10^2–10^6 Hz) using a Hewlett Packard 4194 impedance analyzer.

As shown in figure 4, three different behaviors are observed in dielectric experiments for $Ba_2Pr_xNd_{1-x}FeNb_4O_{15}$ samples.

- For $x = 0$, we observe one sharp peak of ε_r' at about $T = 320$ K with no frequency dispersion as expected for a ferroelectric transition. Let us emphasize that the temperature variation of ε_r' within the paraelectric state at $T > 320$ K is not following the classical Curie–Weiss law as observed in all TTBs [15].
- For $x = 1$, a strong frequency dispersion of ε_r' and ε_r'' occurs whose features fit well with a relaxor transition.
- For $0 < x < 1$, as exemplified in figure 4 for $x = 0.6$, both the high temperature ferroelectric transition and the low temperature relaxor maximum coexist. We note that such a sequence paraelectric–ferroelectric–relaxor states is still a matter of debate in the literature [4, 14, 15].

For all compositions, the high temperature increase of ε_r'' shows the conductivity contribution to the dielectric

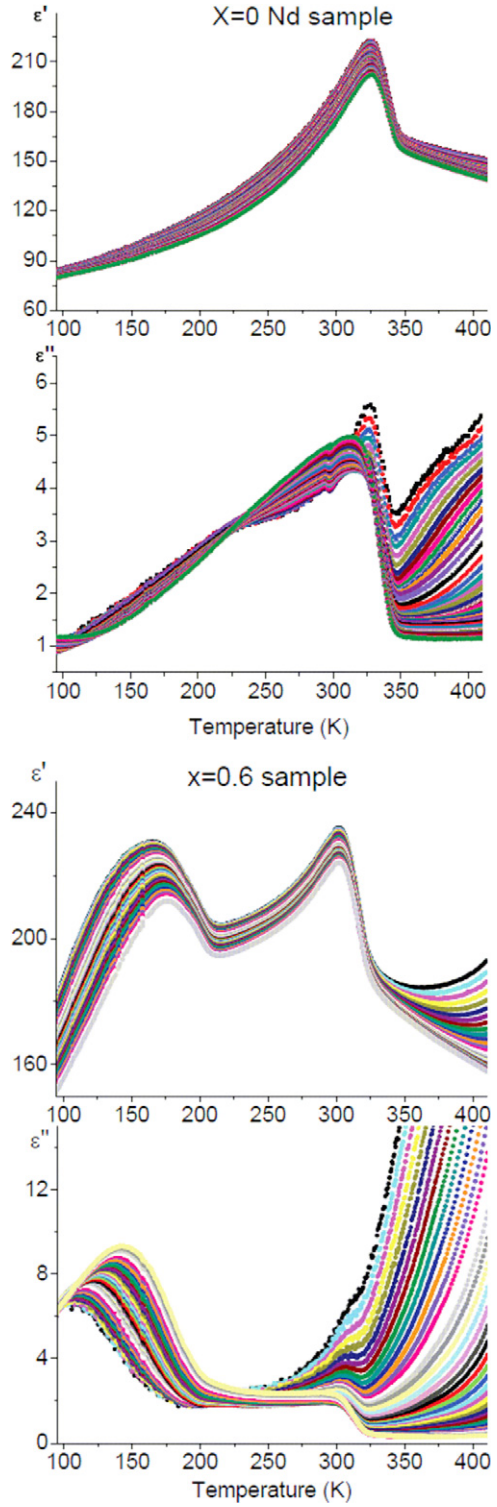

Figure 4. Real (top frame) and imaginary permittivity (bottom frame) for $x = 0$, 0.6 and 1. The operating frequency is scanned from 10^2 to 10^6 Hz from top to bottom. The high temperature increase of ε'' stems from a conductivity contribution.

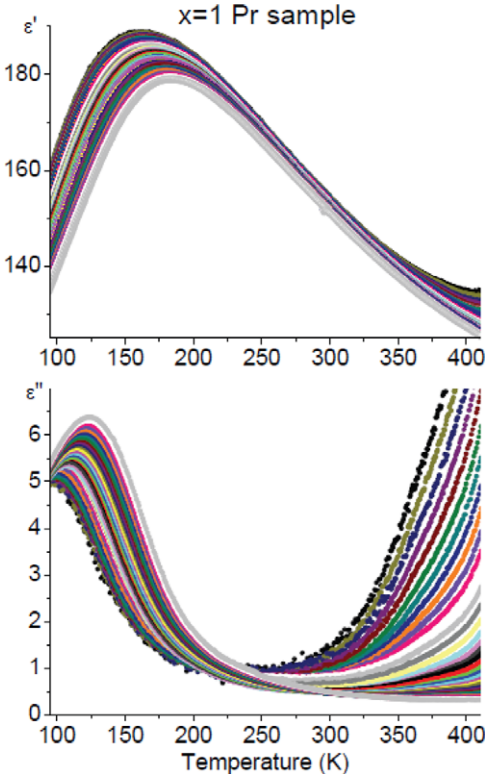

Figure 4. (Continued.)

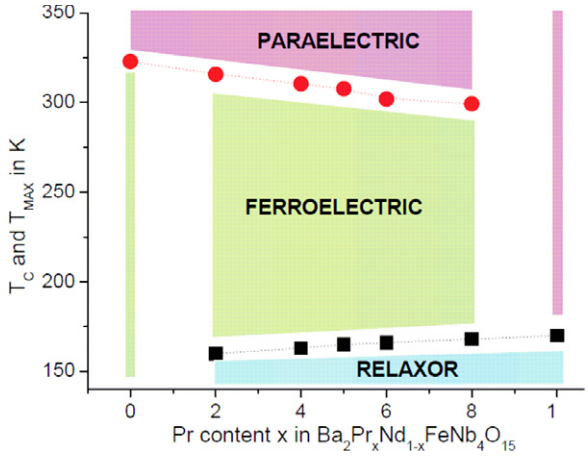

Figure 5. Qualitative phase diagram of $Ba_2Pr_xNd_{1-x}FeNb_4O_{15}$ showing coexistence between ferroelectricity and relaxor state in the intermediate composition range. Note that both the ferroelectric and relaxor temperatures are nearly independent of the composition.

parameters in this temperature range. To underline the stability of the intermediate state, we have plotted in figure 5 the qualitative evolution of the ferroelectric and relaxor temperature (taken at 1 MHz) as a function of x. This shows that, unlike perovskite materials, the Pr/Nd substitution in TTB does not change the ferroelectric much as well as the relaxor temperature. Within this intermediate ferroelectric range, polarization hysteresis loops are recorded with saturated polarization below 1 μC cm^{-2}, which is consistent with what was reported for similar rare-earth-containing TTB [16]. The gradual suppression of ferroelectricity under the introduction of Pr is clearly shown in figure 6 where the hysteresis loops are disappearing on going from the Nd pure phase to the Pr one.

However, not changing the temperature does not mean that the Pr substitution leaves the respective ferroelectric and

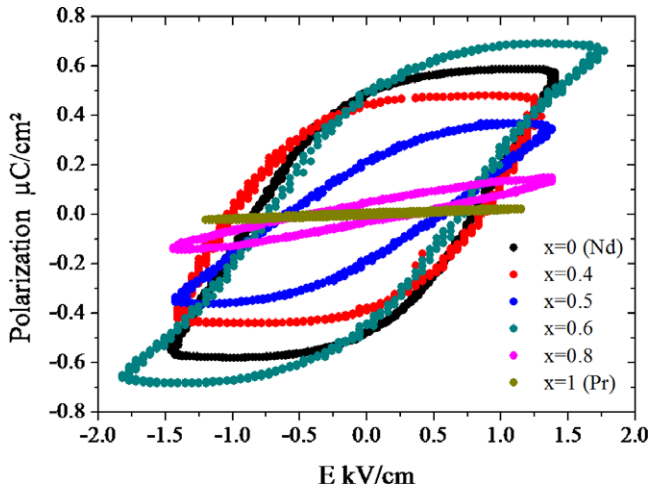

Figure 6. Ferroelectric hysteresis loops at 280 K, evolution of the polarization of the $Ba_2Pr_xNd_{1-x}FeNb_4O_{15}$ samples under 1.6 ± 0.2 kV cm^{-1}.

Table 1. The activation energy E_A and the Vogel–Fulcher temperature T_{VF} versus Pr content x.

x	T_{VF} (K)	E_A (eV)
0	—	—
0.2	152.36	0.03
0.4	149.76	0.024
0.5	149.29	0.031
0.6	141.91	0.053
0.8	128.57	0.089
1	110.16	0.121

relaxor states unaffected. As usual for relaxors, we fitted the low temperature dielectric dispersion using the Vogel–Fulcher equation $\omega = \omega_0 \exp(\frac{E_A}{k_B(T-T_{VF})})$ [17–19].

As shown in table 1, both the activation energy E_A and the Vogel–Fulcher temperature T_{VF} shift continuously with Pr content x. This is also supported by the dispersion which increases strongly in the same time. These changes in the detailed relaxor parameters mean that the microscopic origin of the relaxor state depends on the Pr content. As shown in figure 5, this substitution also alters a lot the ferroelectric transition peak. Indeed, we have plotted (figure 7(a)) in a normalized way the dielectric permittivity for all investigated compositions only for one frequency ($f = 1$ MHz) for the sake of clarity. We clearly see that the ferroelectric peak collapses at a fixed temperature while the relaxor state grows. In the intermediate range, the coexistence of both the ferroelectric and relaxor states stems from a linear superposition of the end member behavior, as confirmed by the computed curves in figure 7(b) where we have used $\varepsilon'_r(x) = x\varepsilon'_r(1) + (1-x)\varepsilon'_r(0)$. The agreement between figures 7(a) and (b) confirms that there are no extra contributions in the intermediate composition range at least for the position and shape of the dielectric peaks. This is rather unusual in ferroelectric materials and TTB are thus more flexible than standard close packed structures like perovskites.

We next want to discuss why the ferroelectric peak collapses without a significant change of the transition

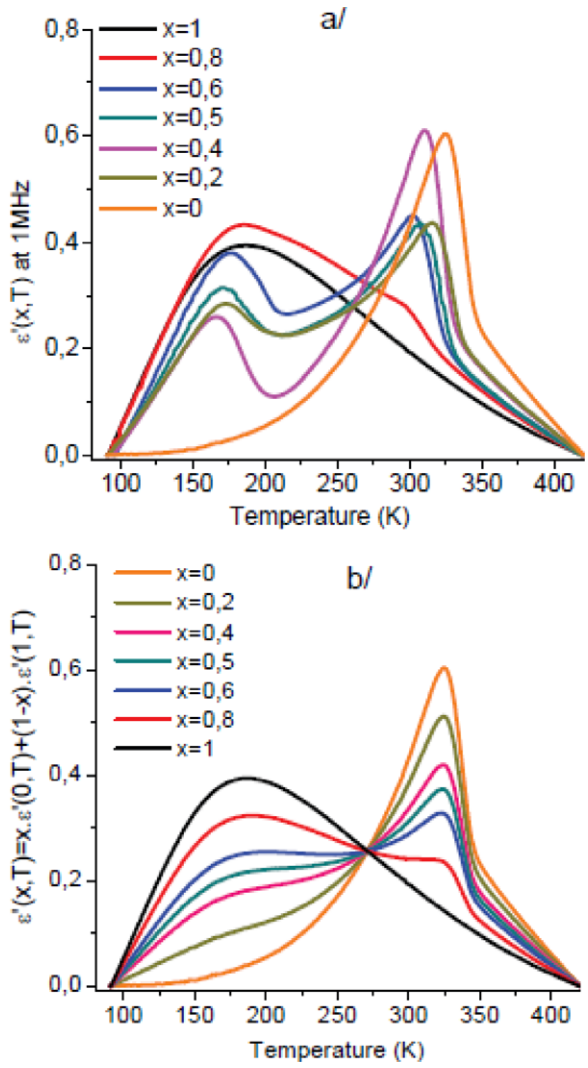

Figure 7. (a) Normalized dielectric data at 1 MHz for the whole set of compositions $Ba_2Pr_xNd_{1-x}FeNb_4O_{15}$ $0 < x < 1$; in (b) the curves for the intermediate compositions $\varepsilon(x, T)$ have been reconstructed by a linear superposition of the end members $\varepsilon(0, T)$ and $\varepsilon(1, T)$.

temperature. Even if the Curie–Weiss law is not valid for TTBs, we can use a very crude approximation to understand why the dielectric maximum decreases while its temperature of occurrence remains. Within a full order–disorder model [20, 21], the Curie constant which fixes the maximum reached ε'_r is related to the density of dipoles in the high temperature paraelectric state. When those dipoles are originating from correlated chains, the Curie constant C is inversely proportional to the density N of correlated chains [22–24]. As a result, one can write $\varepsilon'_r \propto \frac{C}{T-T_C}$ and $C \propto \frac{1}{N}$. If the density of chains decreases, C increases and the maximum reached ε'_r decreases and eventually disappears without affecting the transition temperature T_C. We thus can state that our samples containing only Nd ($x = 0$) have a small density of long chains and a well-defined maximum of ε'_r is recorded. On the other hand, the Pr-containing samples include a high density N of small chains and thus the maximum of ε'_r collapses. We next need to find an origin for this cutting down of ferroelectric correlation chains when the amount

of Pr increases. Such a model is outside the scope of the present communication but we can recall that the suppression of ferroelectric correlation usually results from mass, volume or charge imbalance among substituted cations [25, 26].

Without excluding them, we can state that the mass and volume change under Pr substitution are not the main driving force. Indeed, in such a case, noticeable structural changes as well as strong shifts in the ferroelectric transition temperature are expected and these are not observed here. We thus can look for differences in the electronic states: Pr may carry at least two valences (III and IV) while Nd has a fixed III state. As a consequence, for the sake of neutrality, the valency of Fe which is sitting at the ferroelectric active site within the oxygen octahedron can also be balanced between III and II (or the valency of niobium may change from V to IV). However, preliminary Mössbauer analysis did not show Fe^{2+} in the $x = 1$ ceramics. Whatever the microscopic mechanism, the main outcome of this may be a change in the Nb–O correlation chains and so the polar units will be split and their density N increased. By the way, such a decrease of ferroelectric correlation under increasing Pr content is also able to induce the relaxor low temperature state and the effect that is seen in figures 4 and 7(a) would be fully explained. This very simple model will need further investigation such as by Raman scattering but we stress again the main result that we reported here: the flexibility of the open TTB network allows for a tuning of the ferroelectric to relaxor crossover on scanning the composition from Nd to Pr in $Ba_2Nd_{1-x}Pr_xFeNb_4O_{15}$.

The authors want to thank E Lebraud and S Pechev for the collection of x-ray diffraction data and A Fargues for polishing the samples. This work is supported by the European Network of Excellence 'FAME' (www.famenoe.net) and the STREP MaCoMuFi (www.macomufi.eu).

References

[1] Ma W and Cross L E 2001 *Appl. Phys. Lett.* **78** 2920
[2] Bokov A A and Ye Z-G 2006 *J. Mater. Sci.* **41** 31
[3] Damjanovic D, Budimir M, Davis M and Setter N 2006 *J. Mater. Sci.* **41** 65
[4] Simon A, Ravez J and Maglione M 2004 *J. Phys.: Condens. Matter* **16** 963
[5] Ravez J, Broustéra C and Simon A 1999 *J. Mater. Chem.* **9** 1609
[6] Kreisel J, Glazer A M, Bouvier P and Lucazeau G 2001 *Phys. Rev.* B **63** 174106
[7] Gomah-Pettry J R, Saïd S, Marchet P and Mercurio J P 2004 *J. Eur. Ceram. Soc.* **24** 1165
[8] Simon A, Ravez J and Maglione M 2005 *Solid State Sci.* **7** 925
[9] Magneli A 1949 *Ark. Kem.* **24** 213
[10] Pouchard M, Chaminade J-P, Perron A, Ravez J and Hagenmuller P 1975 *J. Solid State Chem.* **14** 274
[11] Fang P H and Roth R S 1960 *J. Appl. Phys.* **31** 143
[12] Castel E, Josse M, Roulland F, Michau D, Raison L and Maglione M 2009 *J. Magn. Magn. Mater.* **321-11** 1773
[13] Perrin C, Menguy N, Bidault O, Zahra C Y, Zahra A-M, Caranoni C, Hilczer B and Stepanov A 2001 *J. Phys.: Condens. Matter* **13** 10231
[14] Samara G A and Boatner L A 2000 *Phys. Rev.* B **61** 3889
[15] Josse M, Bidault O, Roulland F, Castel E, Simon A, Michau D, Von der Mühll R, Nguyen O and Maglione M 2009 *Solid State Sci.* **11** 1118
[16] Chen I W 2000 *J. Phys. Chem. Solids* **61** 197
[17] Viehland D, Jang S J, Cross L E and Wuttig M 1990 *J. Appl. Phys.* **68** 2916
[18] Vogel H 1921 *Phys. Z.* **22** 645
[19] Fulcher G S 1925 *J. Am. Ceram. Soc.* **8** 339
[20] Jona F and Shirane G 1962 *Ferroelectric Crystals* (New York: MacMillan) pp 152–253
[21] Burns G and Scott B A 1988 *Phys. Rev.* B **38** 597
[22] Comes R, Lambert M and Guinier A 1968 *Solid State Commun.* **6** 715
[23] Quittet A M and Lambert M 1972 *J. Phys. Colloq.* **33** C2–141
[24] Yu R and Krakauer H 1995 *Phys. Rev. Lett.* **74** 4067
[25] Cochran W 1961 *Adv. Phys.* **10** 401
[26] Scott J F 1970 *Phys. Rev.* B **4** 1360